J Syst Sci Complex (2016) 29: 978–990

Full-Order Sliding Mode Control for High-Order Nonlinear System Based on Extended State Observer*

CHEN Qiang · TAO Liang · NAN Yurong

DOI: 10.1007/s11424-016-5141-1
Received: 8 June 2015 / Revised: 8 November 2015

Abstract In this paper, a full-order sliding mode control based on extended state observer (FSMC+ESO) is proposed for high-order nonlinear system with unknown system states and uncertainties. The extended state observer (ESO) is employed to estimate both the unknown system states and uncertainties so that the restriction that the system states should be completely measurable is relaxed, and a full-order sliding mode controller is designed based on the ESO estimation to overcome the chattering problem existing in ordinary reduced-order sliding mode control. Simulation results show that the proposed method facilitates the practical application with respect to good tracking performance and chattering elimination.

Keywords Extended state observer, full-order sliding mode control, high-order nonlinear system.

1 Introduction

High-order nonlinear system is a very common and broad application system, such as the forth-order single-link flexible-joint robotic manipulator system[1], the fifth-order lumped parameter cardiovascular system[2], the seventh-order navigation system[3], and so on. Due to the higher order, the systems are relatively complex and vulnerable to the nonlinear disturbances such as external disturbances and the unknown friction, so that the controllers are difficult to design with good robustness and anti-interference capabilities.

To improve the control performance and robustness of the system, many advanced techniques are applied to the high-order nonlinear system, such as neural adaptive control[4], sliding mode control[5], auto-disturbance rejection control[6], robust control[7], and fuzzy control[8], etc. Among them, the sliding mode control (SMC) method has been widely used to the control systems because of insensitivity to the parameter perturbations and strong robustness. However,

CHEN Qiang · TAO Liang · NAN Yurong
College of Information Engineering, Zhejiang University of Technology, Hangzhou 310023*, China.*
Email: sdnjchq@zjut.edu.cn.
*This research was supported by the National Natural Science Foundation of China under Grant No. 61403343, and the China Postdoctoral Science Foundation funded project under Grant No. 2015M580521.
◇ *This paper was recommended for publication by Editor SUN Jian.*

due to the existence of the excessively high control gain and the sign function, the conventional sliding mode control has a serious chattering problem, which may lead to some serious damages[9]. Therefore, how to weaken the chattering problem in sliding mode control for the high performance nonlinear control system is one of key technical problems to be solved.

To eliminate the chattering problem, a lot of improved sliding mode control methods have been proposed. An adaptive back-stepping sliding mode controller is proposed in [10] to simplify controller design and shorten arrival time, and the radial basis function neural network observer is presented to solve the large external disturbances and parameter uncertainties. Thus, the input chattering in sliding mode control is reduced. In [11], an adaptive sliding mode control method and the auto-tuning scheme of the sliding switching gain are investigated for a three phase UPS system. Through the method, the chattering problem in the sliding mode is greatly weakened and the excessive use of electric power for the overestimation of sliding switching gain is reduced. Lin, et al.[12] proposed an intelligent second-order sliding mode control based on a wavelet fuzzy neural network with an asymmetric membership function estimator for an electric power steering system. The second-order sliding mode control is developed to reduce the chattering problem in traditional sliding mode control, and the experimental results are provided to illustrate the effectiveness of the method.

In order to further eliminate the chattering in sliding mode control, the combination between sliding mode control and auto-disturbance rejection control is proposed in recent years. In [13], a nonsingular fast terminal sliding mode control method based on ESO and the tracking differentiator is presented for an uncertain SISO nonlinear system. The system disturbance can be compensated effectively by using ESO, and a better robustness and less chattering are achieved. In [14], an adaptive sliding mode control method based on ESO is presented for chaotic permanent magnet synchronous motor system. The unknown system states and uncertainties are observed by ESO to relax the restriction that all the system states should be completely measured. The simulation results indicate the chattering is reduced and the robustness of the system is enhanced. In [15], to balance the chattering and the anti-disturbance capacity, three kinds of improved integral sliding mode control schemes are proposed for permanent magnet synchronous motor speed control system. The lumped disturbance is estimated by ESO for the feed-forward compensation, and the chattering problem caused by high control gain is reduced.

Although the literatures described above can weaken the chattering problem to some extent, they still cannot eliminate the chattering in the sliding mode controller. Recently, a chattering-free full-order sliding mode control method is proposed in [16]. Compared with conventional reduced-order sliding mode controller, the controller signal is continuous, and can effectively avoid the chattering problem. But the condition of this method is that all the system states should be completely measurable, which limits its applications in the system with unknown states and uncertainties. Therefore, the design of a chattering-free sliding mode control based on ESO for the system with unknown states and uncertainties is still a challenging work.

In this paper, a full-order sliding mode control based on extended state observer is proposed for high-order nonlinear systems with unknown system states and uncertainties. The unknown system states and uncertainties are estimated by the nonlinear extended state observer, and

the chattering-free full-order sliding mode controller is developed based on the estimation to achieve a high performance without chattering phenomenon.

The rest of this paper is organized as follows. Section 2 briefly describes the high-order nonlinear system. The extended state observer is designed in Section 3. In Section 4, the full-order sliding mode controller is proposed for high-order nonlinear system and the system stability analysis is provided. The simulation example is given in Section 5 and the conclusion is provided in Section 6.

2 System Description

Consider the following general high-order nonlinear system

$$\begin{cases} \dot{x}_1 = x_2, \\ \dot{x}_2 = x_3, \\ \vdots \\ \dot{x}_{n-1} = x_n, \\ \dot{x}_n = f(\boldsymbol{x}, t) + b_0 u, \\ \dot{x}_{n+1} = h, \end{cases} \tag{1}$$

where n is the system order; $\boldsymbol{x} = [x_1, x_2, \cdots, x_n]^{\mathrm{T}}$ denotes the system state vector; $f(\boldsymbol{x}, t)$ is a nonlinear function of system state $\boldsymbol{x}$, which represents the nonlinear characteristics of the system, including the total external disturbance and system parameters uncertainties; u represents the system control input; b is an unknown constant; y is the system output.

The control objective is to design a controller so that the actual output of the system can accurately track the reference trajectory. However, since $f(\boldsymbol{x}, t)$ and b are unknown, the controller cannot be designed directly. Then, an observer should be given first to estimate the unknown states and uncertainties.

Define $a(\boldsymbol{x}, t) = f(\boldsymbol{x}, t) + (b - b_0)u$, where b_0 is the estimation of b, and can be given by experience. According to the idea of ESO[17], define an extended state $x_{n+1} = a(\boldsymbol{x}, t)$, and (1) can be rewritten in the following equivalent form

$$\begin{cases} \dot{x}_1 = x_2, \\ \dot{x}_2 = x_3, \\ \vdots \\ \dot{x}_{n-1} = x_n, \\ \dot{x}_n = f(\boldsymbol{x}, t) + bu, \\ \dot{x}_{n+1} = h \end{cases} \tag{2}$$

with $h = \dot{a}(\boldsymbol{x}, t)$.

3 Extended State Observer Design

Define $z_i, i = 1, 2, \cdots, n+1$, are the observations of system states x_i in (2) and $\varepsilon_i = z_i - x_i$ are the observation errors. Then, the nonlinear extended state observer becomes

$$\begin{cases} \varepsilon_1 = z_1 - x_1, \\ \dot{z}_1 = z_2 - \beta_1 \varepsilon_1, \\ \dot{z}_2 = z_3 - \beta_2 \text{fal}(\varepsilon_1, \alpha_1, \delta), \\ \vdots \\ \dot{z}_{n-1} = z_n - \beta_{n-1} \text{fal}(\varepsilon_1, \alpha_{n-2}, \delta), \\ \dot{z}_n = z_{n+1} - \beta_n \text{fal}(\varepsilon_1, \alpha_{n-1}, \delta) + b_0 u, \\ \dot{z}_{n+1} = -\beta_{n+1} \text{fal}(\varepsilon_1, \alpha_n, \delta), \end{cases} \tag{3}$$

where $\beta_1, \beta_2, \cdots, \beta_{n+1}$ are the observer gains; $\text{fal}(\cdot)$ is a continuous power function which has linear segments in the neighborhood of the origin, and its expression is given as

$$\text{fal}(\varepsilon_1, \alpha_i, \delta) = \begin{cases} \dfrac{\varepsilon_1}{\delta^{1-\alpha_i}}, & |\varepsilon_1| \le \delta, \\ |\varepsilon_1|^{\alpha_i} \text{sign}(\varepsilon_1), & |\varepsilon_1| > \delta, \end{cases} \tag{4}$$

where $i = 1, 2, \cdots, n$; $\delta > 0$ represents the range length of linear segment; $0 < \alpha_i < 1$ is a constant.

Remark 3.1 The system dynamics $f(\boldsymbol{x}, t)$ in System (1) is continuously differentiable and bounded. This assumption is reasonable in the actual system. For example, when the nonlinear characteristic $f(\boldsymbol{x}, t)$ denotes the friction on system, the value of friction is always limited, or the system disturbance and uncertainties also cannot be infinite in practical applications.

Remark 3.2 From the boundedness of $f(\boldsymbol{x}, t)$, it can be concluded that $a(\boldsymbol{x}, t) = f(\boldsymbol{x}, t) + (b - b_0)u$ is bounded. As pointed in [17–19], the nonlinear function $\text{fal}(\cdot)$ can guarantee that observer states z_i tends to x_i by choosing the appropriate parameters β_i, and the observer errors can converge to $|x_i - z_i| \le l_i$, where $l_i > 0$ are small positive numbers.

4 Controller Design and Stability Analysis

In the former sections, the dynamic function of the high-order nonlinear system is described, and the ESO is investigated for the system. In order to achieve the precise tracking for the reference trajectory, in this section, the full-order sliding mode control based on ESO (FSMC+ESO) is designed.

Define the system tracking error e and its different order derivatives are

$$\begin{cases} e = y - y_d = x_1 - y_d, \\ \dot{e} = \dot{x}_1 - \dot{y}_d = x_2 - \dot{y}_d, \\ \ddot{e} = \dot{x}_2 - \ddot{y}_d = x_3 - \ddot{y}_d, \\ \vdots \\ e^{(n-1)} = x_n - y_d^{(n-1)}, \\ e^{(n)} = \dot{x}_n - y_d^{(n)} = x_{n+1} + b_0 u - y_d^{(n)}, \end{cases} \tag{5}$$

where y_d is the reference trajectory.

4.1 Full-Order Sliding Mode Controller Design

Design the full-order sliding mode surface as

$$s = e^{(n)} + \lambda_n e^{(n-1)} + \lambda_{n-1} e^{(n-2)} + \cdots + \lambda_2 \dot{e} + \lambda_1 e, \tag{6}$$

where $\lambda_i > 0, i = 1, 2, \cdots, n$, are the control parameters and chosen such that the polynomial $p^n + \lambda_n p^{n-1} + \cdots + \lambda_2 p + \lambda_1$ is Hurwitz.

Substituting (5) into (6) yields

$$s = x_{n+1} + b_0 u - y_d^{(n)} + \lambda_n (x_n - y_d^{(n-1)}) + \cdots + \lambda_2 (x_2 - \dot{y}_d) + \lambda_1 (x_1 - y_d). \tag{7}$$

From (7), the FSMC+ESO is designed as

$$u = \frac{1}{b_0}(u_{eq} + u_n), \tag{8}$$

$$u_{eq} = -z_{n+1} + y_d^{(n)} - \lambda_n (z_n - y_d^{(n-1)}) - \cdots - \lambda_2 (z_2 - \dot{y}_d) - \lambda_1 (z_1 - y_d), \tag{9}$$

$$\dot{u}_n + T u_n = v, \tag{10}$$

$$v = -k \cdot \mathrm{sign}(s) \tag{11}$$

where $T > 0$, $k = k_p + k_T + \eta$, $\eta, k_p, k_T > 0$ are the control gains.

Remark 4.1 In (8)–(11), the controller u consists of two parts: u_{eq} is an equivalent controller and u_n is the output of the low-pass filter in (10), whose transfer function can be expressed as $U_n(s)/V(s) = 1/(s+T)$. Although v is a non-smooth function with the sliding mode switch $\mathrm{sign}(s)$ in (11), u_n is a smooth function by passing the low-pass filter. Therefore, the actual control signal u does not include any switch item directly, and the traditional chattering problem caused by the switch function can be avoided.

Substituting (8)–(11) into (7) gives

$$s = u_n + p(\boldsymbol{x}, \boldsymbol{z}), \tag{12}$$

where $p(\boldsymbol{x}, \boldsymbol{z}) = (x_{n+1} - z_{n+1}) + \lambda_n (x_n - z_n)) + \cdots + \lambda_2 (x_2 - z_2) + \lambda_1 (x_1 - z_1)$, and satisfies the condition that $p(\boldsymbol{x}, \boldsymbol{z}) \le l_p$ with $l_p = l_{n+1} + \lambda_n l_n + \cdots + \lambda_2 l_2 + \lambda_1 l_1$.

Differentiating (12) yields

$$\dot{s} = \dot{p}(\boldsymbol{x}, \boldsymbol{z}) + (k_p + k_T + \eta)\mathrm{sign}(s) - T u_n. \tag{13}$$

4.2 Stability Analysis

Lemma 4.2 (see [20]) *Suppose that a continuous, positive-definite function $V(t)$ satisfies the following differential inequality:*

$$\dot{V}(t) \leq -\alpha V^{\beta}(t), \quad \forall t \geq t_0,\ V(t_0) \geq 0, \tag{14}$$

where $\alpha > 0$, $0 < \eta < 1$ are constants. Then, for any given t_0, $V(t)$ satisfies the following inequality:

$$V^{1-\beta}(t) \leq V^{1-\beta}(t_0) - \alpha(1-\beta)(t-t_0), \quad t_0 \leq t \leq t_1 \tag{15}$$

and

$$V(t) \equiv 0, \quad \forall t \geq t_1 \tag{16}$$

with t_1 given by $t_1 = t_0 + \frac{V^{1-\beta}(t_0)}{\alpha(1-\beta)}$.

Theorem 4.3 *Considering the high-order nonlinear system* (1)*, the full order sliding mode* (6)*, and the controller* (8)–(11)*, the sliding mode surface s can converge to zero in finite time and the tracking error e can stably converge to zero when the control parameters k_p and k_T satisfy the conditions that $k_p \geq |\dot{p}(\boldsymbol{x}, \boldsymbol{z})|$ and $k_T \geq Tl_p$.*

Proof Define the following Lyapunov function

$$V = \frac{1}{2}s^2. \tag{17}$$

Differentiating (17), and from (8)–(11), the dynamics is

$$\begin{aligned}
\dot{V} = s\dot{s} &= s(\dot{p}(\boldsymbol{x}, \boldsymbol{z}) + v - Tu_n) \\
&= (\dot{p}(\boldsymbol{x}, \boldsymbol{z}) - k_p|s|) + (-Tu_n s - k_T|s|) - \eta|s| \\
&= (\dot{p}(\boldsymbol{x}, \boldsymbol{z}) - k_p|s|) + (-Ts^2 + Tp(\boldsymbol{x}, \boldsymbol{z})s - k_T|s|) - \eta|s| \\
&\leq (\dot{p}(\boldsymbol{x}, \boldsymbol{z}) - k_p|s|) + (-Ts^2 + Tl_p s - k_T|s|) - \eta|s|.
\end{aligned} \tag{18}$$

When the parameters k_p and k_T are chosen to satisfy $k_p \geq |\dot{p}(\boldsymbol{x}, \boldsymbol{z})|$ and $k_T \geq Tl_d$, respectively, it can be concluded as

$$\dot{V} = s\dot{s} \leq -\eta|s| < 0. \tag{19}$$

From (19), one obtains the following relationship: $\dot{V} \leq -\beta_m V^{\frac{1}{2}}$ with $\beta_m = \eta 2^{\frac{1}{2}}$. According to Lemma 4.2, there is a limited time t_2 to satisfy the condition $t \geq t_2$, which can can guarantee that sliding mode surface s has a fast convergence to zero in finite time. Since the polynomial $p^n + \lambda_n p^{n-1} + \cdots + \lambda_2 p + \lambda_1$ is Hurwitz, the tracking error e can be guaranteed to asymptotically converge to zero. This completes the theorem proof. ∎

5 Simulation Results

In Section 4, the full-order sliding mode controller based on ESO is designed to achieve effective tracking performance for reference trajectory. In this section, a fourth-order single-link

flexible-joint robotic manipulator system is provided to evaluate the effectiveness and superior performance of the proposed control method.

The dynamic equations of the four order single-link flexible-joint robotic manipulator system is taken from [1], and can be described as

$$\begin{cases} I\ddot{q}_1 + MgL\sin(q_1) + K(q_1 - q_2) = 0, \\ J\ddot{q}_2 - K(q_1 - q_2) = u, \end{cases} \tag{20}$$

where q_1 and q_2 are the angles of the link and motor, respectively; I denotes the inertia of the link; J represents the motor inertia; K is the stiffness of the spring; M and L are the math and length of the link, respectively; and u is the control torque. The output of the system is $y = q_1$.

Define $x_1 = q_1$, $x_2 = \dot{q}_1 = \dot{x}_1$, $x_3 = q_2$, $x_4 = \dot{q}_2 = \dot{x}_3$, and the system (20) is rewritten as

$$\begin{cases} \dot{x}_1 = x_2, \\ \dot{x}_2 = -\dfrac{MgL}{I}\sin x_1 - \dfrac{K}{I}(x_1 - x_3), \\ \dot{x}_3 = x_4, \\ \dot{x}_4 = \dfrac{K}{J}(x_1 - x_3) + \dfrac{1}{J}u. \end{cases} \tag{21}$$

For the convenience of using ESO, define $\overline{x}_1 = x_1$, $\overline{x}_2 = x_2$, $\overline{x}_3 = -\frac{MgL}{I}\sin x_1 - \frac{K}{I}(x_1 - x_3)$, $\overline{x}_4 = -x_2\frac{MgL}{I}\cos x_1 - \frac{K}{I}(x_2 - x_4)$, and (21) is transformed into

$$\begin{cases} \dot{\overline{x}}_1 = \overline{x}_2, \\ \dot{\overline{x}}_2 = \overline{x}_3, \\ \dot{\overline{x}}_3 = \overline{x}_4, \\ \dot{\overline{x}}_4 = a(\overline{\boldsymbol{x}}) + bu, \end{cases} \tag{22}$$

where $a(\overline{\boldsymbol{x}}) = \frac{MgL}{I}\sin(\overline{x}_1)(\overline{x}_2^2 - \frac{K}{J}) - (\frac{MgL}{I}\cos(\overline{x}_1) + \frac{K}{J} + \frac{K}{I})\overline{x}_3$, $b = \frac{K}{IJ}$.

Define the extended state $\overline{x}_5 = b(\overline{\boldsymbol{x}})$, where $b(\overline{\boldsymbol{x}}) = a(\overline{\boldsymbol{x}}) + (b - b_0)u$, the coordinate transformation of (22) is given as

$$\begin{cases} \dot{\overline{x}}_1 = \overline{x}_2, \\ \dot{\overline{x}}_2 = \overline{x}_3, \\ \dot{\overline{x}}_3 = \overline{x}_4, \\ \dot{\overline{x}}_4 = \overline{x}_5 + b_0 u, \\ \dot{\overline{x}}_5 = h, \end{cases} \tag{23}$$

where $h = \dot{b}(\overline{\boldsymbol{x}})$.

According to (8)–(11), the FSMC+ESO is designed as

$$u = \frac{1}{b_0}(u_{eq} + u_n), \tag{24}$$

$$u_{eq} = -z_5 + y_d^{(4)} - \lambda_4(z_4 - y_d) - \lambda_3(z_3 - \ddot{y}_d) - \lambda_2(z_2 - \dot{y}_d) - \lambda_1(z_1 - y_d), \tag{25}$$

$$\dot{u}_n + Tu_n = v, \tag{26}$$

$$v = -k \cdot \text{sign}(s), \tag{27}$$

where $T \geq 0$, $k = k_p + k_T + \eta$, $\eta > 0$, $k_p > 0$, $k_T > 0$ are the control gains.

Define the reduced-order sliding mode as

$$\begin{aligned} s_1 &= e^{(3)} + \phi_3 \ddot{e} + \phi_2 \dot{e} + \phi_1 e \\ &= \overline{x}_4 - y_d^{(3)} + \phi_3(\overline{x}_3 - \ddot{y}_d) + \phi_2(\overline{x}_2 - \dot{y}_d) + \phi_1(\overline{x}_1 - y_d). \end{aligned} \tag{28}$$

Differentiating (28) yields

$$\begin{aligned} \dot{s}_1 &= e^{(4)} + \phi_3 e^{(3)} + \phi_2 \ddot{e} + \phi_1 \dot{e} \\ &= \overline{x}_5 + b_0 u - y_d^{(4)} + \phi_3(\overline{x}_4 - y_d^{(3)}) + \phi_2(\overline{x}_3 - \ddot{y}_d) + \phi_1(\overline{x}_2 - \dot{y}_d). \end{aligned} \tag{29}$$

According to (29), the RSMC+ESO can be designed as

$$u_s = \frac{1}{b_0}(-z_5 + y_d^{(4)} - \phi_3(z_4 - y_d^{(3)}) - \phi_2(z_3 - \ddot{y}_d) - \phi_1(z_2 - \dot{y}_d) - k_1 \cdot \text{sign}(s_1)). \tag{30}$$

In this simulation, all the control parameters are fixed. Set the initial states as $x_1(0) = x_2(0) = x_3(0) = x_4(0) = x_5(0) = 0$, $z_1(0) = z_2(0) = z_3(0) = z_4(0) = z_5(0) = 0$; the system parameters are $MgL = 10$, $K = 100$, $I = J = 1$; the ESO parameters are given by $\beta_1 = 200$, $\beta_2 = 1.5 \times 10^4$, $\beta_3 = 5.8 \times 10^5$, $\beta_4 = 5 \times 10^6$, $\beta_5 = 1.5 \times 10^8$, $\alpha_1 = 0.5$, $\alpha_2 = 0.25$, $\alpha_3 = 0.125$, $\alpha_4 = 0.0625$, $\delta = 0.1$; the control parameters are $\lambda_1 = 1.8 \times 10^4$, $\lambda_2 = 5000$, $\lambda_3 = 800$, $\lambda_4 = 20$, $\phi_1 = 2400$, $\phi_2 = 400$, $\phi_3 = 15$, $k = k_1 = 300$, $T = 1$.

5.1 Case 1: Tracking Performance of $\theta_{ref1} = 0.1\sin(\pi t)$

In this case, the reference trajectory is given as $\theta_{ref1} = 0.1\sin(\pi t)$. The simulation results of tracking reference trajectory and tracking errors for FSMC+ESO and RSMC+ESO are shown in Figures 1 and 2, respectively. Figure 3 provides the control signals of two control methods. Figures 4 and 5 are the observer errors. From Figures 1 and 2, we can see that the steady-state tracking error of FSMC+ESO is slightly larger than RSMC+ESO (about 1.1×10^{-4}rad). But the steady-state control signal of RSMC+ESO is between -4.2 rad and 4.2 rad, while FSMC+ESO is between -0.98 rad and 0.98 rad. It's easy to see that the chattering of RSMC+ESO is much more serious than FSMC+ESO in Figure 3. Since there is no sliding mode switch in the actual control law (24), FSMC+ESO has no chattering in the control signal. The control signal of the RSMC+ESO has a severe chattering because the control law (30) includes the sliding mode switch directly. It means that through a small sacrifice in steady-state tracking error, a control signal with no chattering problem can be obtained. The observer states of ESO have a slight chattering in the initial stage due to the excessively high gains, which lead to a slight chattering of the control signals in the initial time in Figure 3. FSMC+ESO will achieve steady-state with no chattering after 2.7s, while RSMC+ESO will sustain chattering in the whole process.

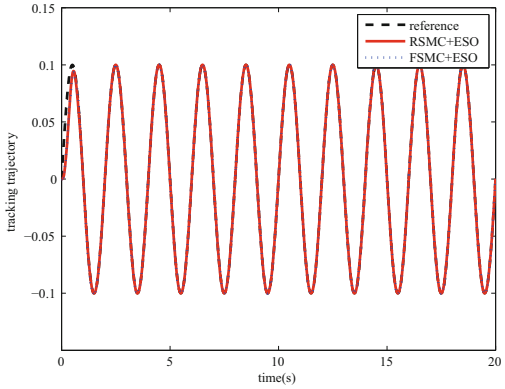

Figure 1 Tracking trajectories for θ_{ref1}

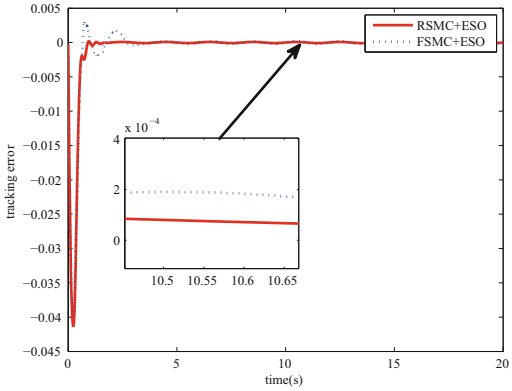

Figure 2 Tracking errors for θ_{ref1}

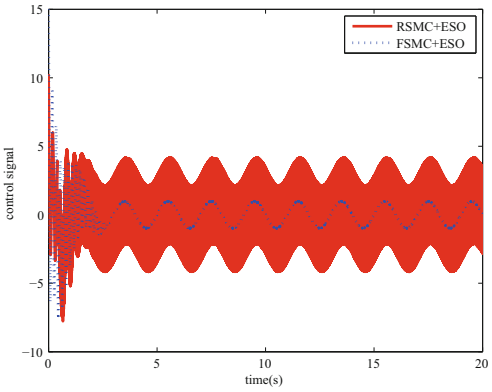

Figure 3 Control signals for θ_{ref1}

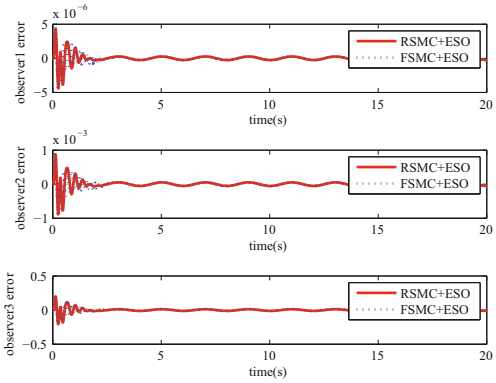

Figure 4 Observer 1–3 errors for θ_{ref1}

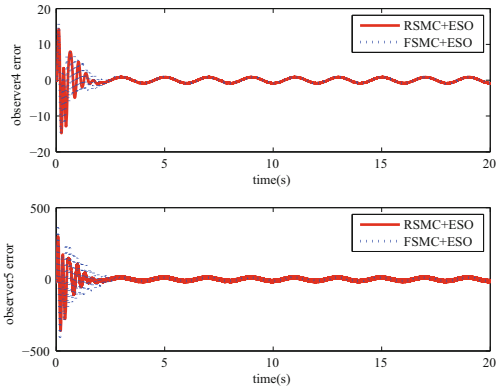

Figure 5 Observer 4–5 errors for θ_{ref1}

In order to satisfy the condition that $k_p \geq |\dot{p}(\boldsymbol{x}, \boldsymbol{z})|$ and $k_T \geq Tl_p$, the following four indices are presented to discuss the selection of parameter k ($k = k_p + k_T + \eta$).

1) The integrated absolute tracking error: IAE= $\int |e(t)|dt$, which is used to describe the system tracking performance.

2) The integrated square tracking error: ISDE= $\int (e(t) - e_0)^2 dt$, which is taken to indicate the fluctuations of the track error, where e_0 is the mean value of the tracking error.

3) The integrated absolute control torque: IAU= $\int |u(t)|dt$, which is used to measure the overall amount of control torque.

4) The integrated square control torque: ISDU= $\int (u(t) - u_0)^2 dt$, which is taken to show the fluctuations of control torque, where u_0 is the mean value of the control torque.

As shown in Table 1, the four indices getting smaller and smaller when selecting k within 10 to 10000. However, if k is selected too small (e.g., $k = 10$), the integrated absolute error (IAE) and integrated square error (ISDE) are larger, which means that the tracking performance becomes worse than the case of $k = 100$ to 10000. On the contrary, if k is chosen too large (e.g., $k = 100000$), all the four indices will become larger, which means both tracking performance and chattering-free property in the controller are deteriorated. From Table 1, we can see that the proposed control scheme has a good insensitivity characteristic to the selection of the parameter k, and in order to guarantee good tracking performance and chattering-free property, the value of k could be chosen within the range of 100 to 10000.

Table 1 Four indices comparison of parameter k

	$k = 10$	$k = 100$	$k = 1000$	$k = 10000$	$k = 100000$
IAE	0.0422	0.0231	0.0168	0.0157	0.0224
ISDE	4.6792	4.2659	4.0079	3.1486	3.7610
IAU	18.1494	17.5073	15.5183	13.8234	15.9144
ISDU	39.7120	37.4603	28.0174	17.8165	22.7438

5.2 Case 2: Tracking Performance of $\theta_{ref2} = 0.4\sin(2t) + 0.2\cos(t)$

Without loss of generality, a combination of sine and cosine signals $\theta_{ref2} = 0.4\sin(2t) + 0.2\cos(t)$ is simulated for the comparison of two control methods. All the control parameters and system parameters remain unchanged. Figure 6 is the tracking trajectory and Figure 7 are the tracking errors. The control signals of the two control methods are shown in Figure 8. Figure 9 and Figure 10 provide the observer errors of ESO. As can be seen from Figures 6 and 7, FSMC+ESO has a fast transient response than RSMC+ESO, and the transient response of RSMC + ESO is deteriorated after changing reference trajectory. Therefore, FSMC + ESO has a better robustness than RSMC+ESO. Moreover, the steady-state tracking error of RSMC+ESO is slightly less than FSMC+ESO (about 1.0×10^{-4}rad). From Figure 8, we can see that the control signal of RSMC+ESO has a larger chattering than FSMC+ESO. The FSMC+ESO has a chattering in the initial time because of the excessively higher gains of the

ESO, but the control signal is without chattering anymore when achieving steady-state at 4.7s. However, the control signal of RSMC+ESO is always oscillating within a wide range.

From the simulation results of the example, it can be observed that FSMC+ESO method can achieve a good tracking performance with better robustness and can effectively eliminate the chattering phenomenon in the control signal.

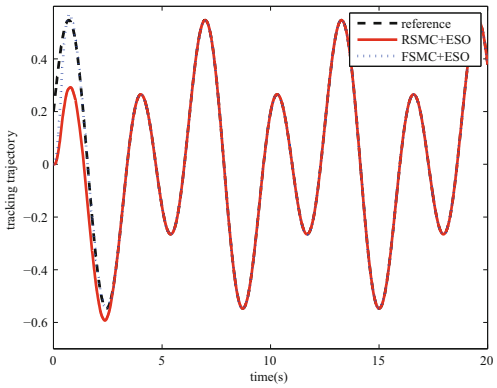

Figure 6 Tracking trajectories for θ_{ref2}

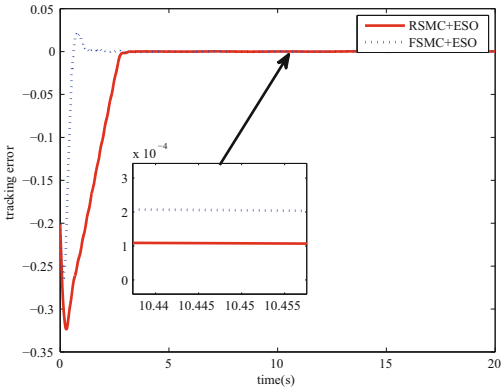

Figure 7 Tracking errors for θ_{ref2}

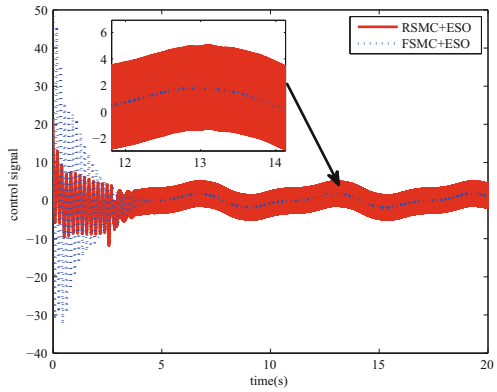

Figure 8 Control signals for θ_{ref2}

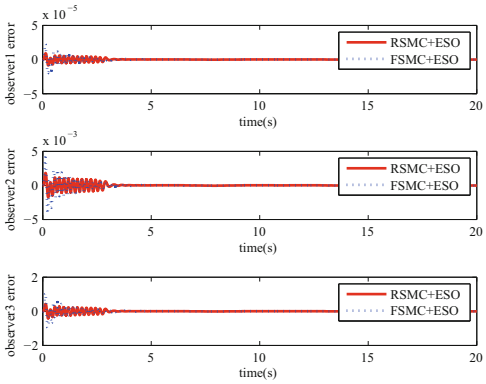

Figure 9 Observer 1–3 errors for θ_{ref2}

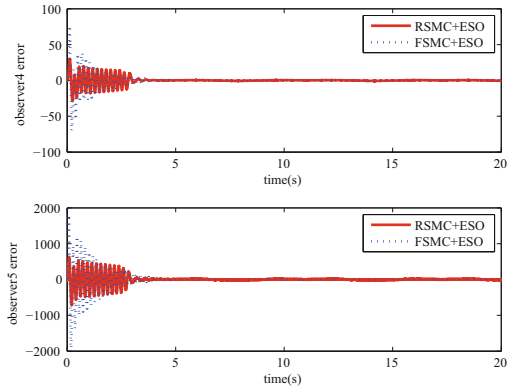

Figure 10 Observer 4–5 errors for θ_{ref2}

6 Conclusion

This paper proposes a full-order sliding mode control method based on extended state observer for high-order nonlinear system. The system unknown states and uncertainties are estimated by the extended state observer. And the full-order sliding mode control strategy is designed based on the estimation, which can guarantee that the output of the system can accurately track the reference trajectory. The simulation results show that FSMC+ESO method has a good steady tracking accuracy without chattering in the control signal, so it facilitates to the practical applications.

References

[1] Talole S E, Kolhe J P, and Phadke S B, Extended-state-observer-based control of flexible-joint system with experimental validation, *IEEE Transactions on Industrial Electronics*, 2010, **57**(4): 1411–1419.

[2] Liu L L, Li L, and Qian K X, Modeling and simulation of a fifth-order lumped parameter cardiovascular system, *Chinese Journal of Biomedical Engineering*, 2012, **31**(1): 13–19.

[3] Krempasky J J, Closed-form solution of seventh-order navigation system for unaided flyout, *Journal of Guidance Control and Dynamics*, 2000, **23**(6): 1072–1076.

[4] Gao S G, Dong H R, Ning B, et al., Neural adaptive control for uncertain nonlinear system with input saturation: State transformation based output feedback, *Neurocomputing*, 2015, **159**(2): 117–125.

[5] Ginoya D, Shendge P D, and Phadke S B, Disturbance observer based sliding mode control of nonlinear mismatched uncertain systems, *Communications in Nonlinear Science and Numerical Simulation*, 2015, **26**(1–3): 98–107.

[6] Cheng C, Hu Y, Wu J, et al., Auto disturbance rejection controller for non-affine nonlinear systems with adaptive observers, *Control Theory and Applications*, 2014, **31**(2): 148–158.

[7] Kapustyan V and Maksimov V, On attaining the prescribed quality of a controlled fourth order system, *International Journal of Applied Mathematics and Computer Science*, 2014, **24**(1): 75–78.

[8] Wu T S, Karkoub M, Chen C T, et al., Robust tracking design based on adaptive fuzzy control of uncertain nonlinear MIMO systems with time delayed states, *International Journal of Control, Automation, and Systems*, 2013, **11**(6): 1300–1313.

[9] Panchade V M, Chile R H, and Patre B M, A survey on sliding mode control strategies for induction motors, *Annual Reviews in Control*, 2013, **37**(2): 289–307.

[10] Wu Y J, Liu B T, Zhang W L, et al., Adaptive backstepping sliding mode controller for flight simulator based on RBFNN, *International Journal of Modeling, Simulation, and Scientific Computing*, 2013, **4**(4): 1342007-1-14.

[11] Choi Y S, Choi H H, and Jung J W, An adaptive sliding-mode control technique for three-phase UPS system with auto-tuning of switching gain, *Electrical Engineering*, 2014, **96**(4): 373–383.

[12] Lin F J, Hung Y C, and Ruan K C, An intelligent second-order sliding-mode control for an electric power steering system using a wavelet fuzzy neural network, *IEEE Transactions on Fuzzy Systems*, 2014, **22**(6): 1598–1611.

[13] He Z X, Liu C T, Zhan Y, et al., Nonsingular fast terminal sliding mode control with extended state observer and tracking differentiator for uncertain nonlinear systems, *Mathematical Problems in Engineering*, 2014, **2014**: 639707-1-16.

[14] Chen Q, Nan Y R, and Xing K X, Adaptive sliding-mode control of chaotic permanent magnet synchronous motor system based on extended state observer, *Acta Physica Sinica*, 2014, **63**(22): 220506-1-8.

[15] Xia C J, Wang X C, Li S H, et al., Improved integral sliding mode control methods for speed control of PMSM system, *International Journal of Innovative Computing Information and Control*, 2011, **7**(4): 1971–1982.

[16] Feng Y, Han F L, and Yu X H, Chattering-free full-order sliding-mode control, *Automatica*, 2014, **50**(4): 1310–1314.

[17] Han J Q, *Active Disturbance Rejection Control Technique*, National Defense Industry Press, Beijing, 2008, 197–201.

[18] Huang Y and Xue W C, Active disturbance rejection control: Methodology and theoretical analysis, *ISA Transaction*, 2014, **53**(4): 963–976.

[19] Gao Z Q, On the centrality of disturbance rejection in automatic control, *ISA Transaction*, 2014, **53**(4): 850–857.

[20] Chen Q, Yu L, and Nan Y R, Finite-time tracking control for motor servo systems with unknown dead-zones, *Journal of Systems Science and Complexity*, 2013, **26**(6): 940–956.